VPS VIBRATIONS IN PHYSICAL SYSTEMS

DOI: 10.21008/j.0860-6897.2023.2.24
Vibrations in Physical Systems, 2023, 34(2), 2023224

# Registration, modal decomposition and analysis of human left ventricles

**Witold STANKIEWICZ**

Poznan University of Technology, Institute of Applied Mechanics, ul. Jana Pawła II 24, 60-965 Poznań, Poland

**Corresponding author:** Witold STANKIEWICZ, email: witold.stankiewicz@put.poznan.pl

**Abstract** Cardiovascular diseases, especially myocardial infarction and heart failure, are among the most common causes of death. Proper, timely diagnosis can be a key factor in reducing the mortality of these diseases. In the present paper, statistical data analysis of left ventricle of human heart is presented. Raster DICOM images are processed, segmented and registered, in order to mark the left ventricle on medical images, and then to obtain its geometrical 3D models of constant topology. Registered, geometrical data, obtained for whole cardiac cycle of patients with healthy hearts, hypertrophy and heart failure, is then decomposed using Principal Component Analysis. The obtained modes represent the movement of the ventricle during one heart cycle. The proposed approach allows neglecting unimportant, noisy signal and enables the interpretation of the heart cycle. It is shown that modal decomposition might be used to distinguish the hearts with heart failure and the group containing healthy hearts and the ones with hypertrophy. Being a non-invasive method, this approach enables the diagnosis of various hearts, including prenatal ones.

**Keywords:** principal component analysis, modal decomposition, ventricle, segmentation, registration.

## 1. Introduction

Cardiovascular diseases, like myocardial infarction, heart failure, cardiomyopathy, angina and arrhythmia are the leading cause of death in European Union. According to Eurostat [1], there were 1.68 million of deaths resulting from such diseases in 2018, which was equivalent to 37.1% of all deaths. This share ranged from about 22.6% to 65.8%, which shows the importance of proper prevention, diagnosis and treatment of cardiovascular diseases, especially the most dangerous of them - myocardial infarction and heart failure.

Among available heart diagnosis techniques, Magnetic Resonance Imaging (MRI) is both non-invasive and provides high quality imaging data, making it preferable approach in diagnosis [2]. Cardiac MRI is recommended (for various scenarios) in the most of the guidelines of European Society of Cardiology [3].

In order to facilitate the analysis of 3D+t images of cardiac cycle, Principal Component Analysis (PCA) might be applied. This method, widely used in unsupervised machine learning technique of model order reduction, enables spatio-temporal separation of the input data into spatial modes and temporal coefficients, which facilitates the analysis of complex, time-varying multidimensional signals. Modal decomposition resulting from PCA enables further interpretation of the cardiac cycle and is a step towards computer-assisted diagnosis. PCA requires the data to be registered: each snapshot - subset of data representing the same state in cardiac cycle - is required to have the same topology. Registration of the data from medical imaging is a subject of continuous research - a surveys of recent works might be found in Viergever et al. [4], Zhou et al. [5] and Ker et al. [6]. Recent research is based on the applications of machine learning [7, 8].

In this paper, the focus is placed on the image processing-based segmentation and registration and modal analysis of medical data from MRI of human heart's left ventricle. An in-house segmentation procedure was developed to mark the left ventricle on MRI images. Then, during the registration, the contour of the left ventricle is determined on each image, which - regardless of the tissue surface area and its shape in a given section - is described using a curve and a set of points with the same topology. The data prepared in this way, for a group of 44 patients (healthy and with heart disease), is analyzed using PCA.

The considered heart diseases are hypertrophy and heart failure, with or without myocardial infarction. Heart failure (HF) is a state, when the heart is unable to provide sufficient blood flow to meet metabolic requirements or accommodate systemic venous return. It might be caused by hypertension, coronary artery disease, infarction (heart attack) and diabetes. Another etiologies include cardiomyopathies, valvular disease, myocarditis, infections, systemic toxins, and cardiotoxic drugs [9].

Myocardial infarction, occurs when blood flow to the heart is decreased or stopped, causing damage to the heart muscle [10]. Its most common cause is a rupture of atherosclerotic plaque on the artery that supplies the heart muscle, which can lead to the formation of blood clots blocking the artery [11]. The obesity, diabetes, hypertension and smoking, as well as advanced age and genetic abnormalities, are among the most important risk factors of atherosclerosis.

Left ventricular hypertrophy (LVH) is associated with an increase in the thickness of the ventricular wall, accompanied by remodeling of the muscle structure. Over time, it might lead to decreased cardiac contractility due to degenerative changes, causing heart failure, myocardial ischemia, arrythmia, cerebrovascular disease and cardio-vascular mortality. It might be caused by hypertension, aortic valve stenosis and diabetes mellitus [12].

## 2. Materials and methods

### 2.1. Data source

In the present study, data from the "Sunnybrook Cardiac Data" (SCD) collection [13] is used. The dataset contains four-dimensional DICOM image sequences showing left ventricles of 45 male and female patients, aged 23 to 88 years, obtained from 3D+t cine Magnetic Resonance Imaging. In the collection there are nine healthy hearts, as well as the ones with hypertrophy (12 patients) and heart failure (with and without myocardial infarction; 12 hearts each). Each of the hearts in the dataset is described by several images (each with a resolution of 256x256 pixels) captured from consecutive parallel sections, perpendicular to the long axis at the level of mid left ventricle. Sample images for 12 consecutive sections and the same heart cycle phase are shown in Fig. 1, while heart cycle of each patient is written using a sequence of 20 images.

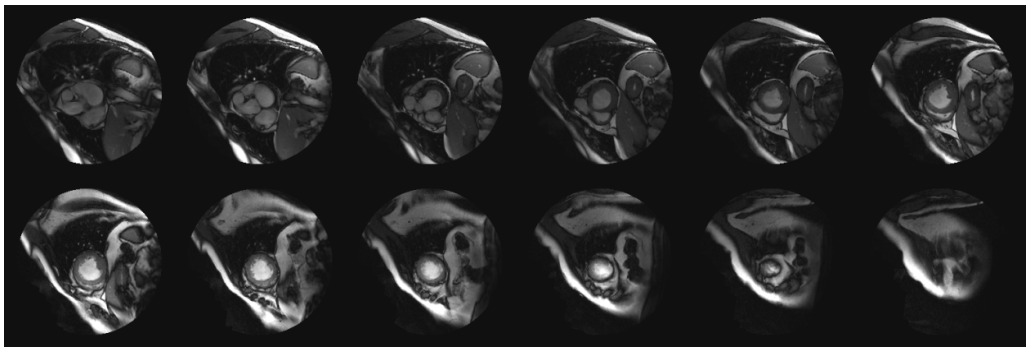

**Figure 1.** DICOM images from the SCD collection - a patient with heart failure.

The aforementioned dataset also contains registered and segmented heart data in the form of prolate spheroid models of left ventricles (Fig. 2), described by the points lying on the intersection of ventricle's surface and consecutive concentric planes, perpendicular to the slices from DICOM data and passing through the centers of outermost contours. Their location is described as a function of cycle phase.

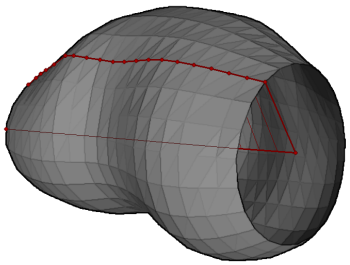

**Figure 2.** Registered left ventricle from the SCD collection - a patient with heart failure; red line connects points lying on the single concentric plane, coinciding with the long axis.

Prolate spheroid models from SCD dataset have already been analyzed using PCA. In the paper [14] modal decompositions have been done for each patient separately - basing on 20 frames from hearts cycle. That approach resulted in the different mode set for each of the patients, and the eigenvalues of the autocorrelation matrices have been used to distinguish healthy hearts from the failure ones.

In this paper, different approach is used to perform the same task. 3D models of the left ventricle for all patients from SCD collection are created using in-house, proprietary algorithms for segmentation and

registration, which allows the processing of data coming directly from medical imaging. Then, the entire set of spatio-temporal models of left ventricles, covering all patients, is used as input for Principal Component Analysis. This results in a different interpretation of data from modal decomposition.

### 2.2. Segmentation and registration of input data

For further statistical (modal) analyses, the tissue of left ventricle has to be identified, and the contours of its shape have to be found for each state of the heart cycle, on each analyzed slice. This procedure is called registration of the data.

In current paper, the registration and segmentation are done using in-house software based on SciPy (Interpolate) and OpenCV libraries [15, 16]. The procedure reads DICOM data and stores it as a series of pixmaps, describing temporal changes over heart contraction-relaxation cycle, for each of analyzed slices. The images are de-noised using anisotropic diffusion [17]. It is a filter based on partial differential equations that uses a thresholding function to prevent the diffusion through the edges, and thus preserving them. The whole segmentation procedure is briefly presented in Fig. 3, and the steps of this procedure are described below. The user specifies approximate coordinates of the center of the tissue of interest (e.g. left ventricle) and enters them to the program, which reads pixel intensities in the vicinity of these coordinates. This enables the adjustment of brightness and contrast of the image to compensate potential differences due to various data sources. After such pre-processing, it is possible to threshold the image to obtain monochromatic bitmap. Then, median blur filter [18] is applied to smooth the image. It is used to remove the noise, to neglect small shapes/spots and to obtain consistent shape of the object on a given section plane for a given phase of the heart cycle. While removing noise, median filtering preserves edges existing in the image.

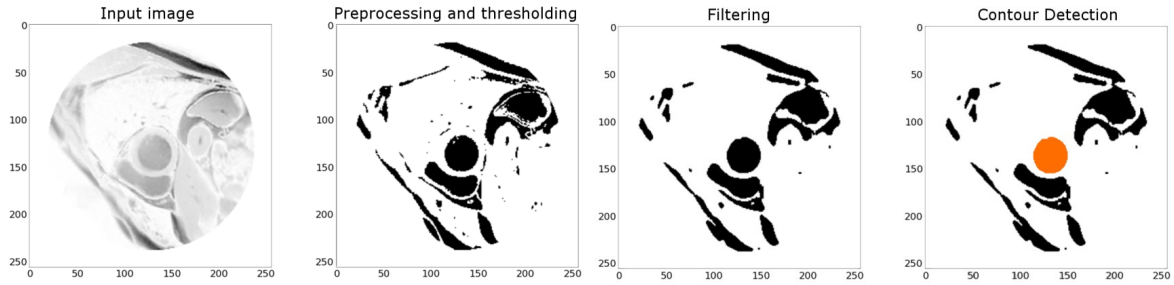


**Figure 3.** Steps of data registration. From left to right: input, image after preprocessing and thresholding, median-filtering, detected contour.

The filter replaces intensity of a given pixel by a median of the values of neighbor pixels, called window. In present study, window of size 5 × 5 pixels is used. Resulting, filtered image is used to detect the contour of the ventricle.

To ensure better fitness of the detected contour and observed tissue's shape, and to avoid blending of adjacent areas, three thresholding variants, based on different value of threshold, are used. For each of the variants, after filtering, the contour on binary image is detected using the procedure findContours from OpenCV [19]. The contour with the center closest to the aforementioned approximate coordinates of the center of the tissue is selected, and it's moments are calculated:

$$m_{ij} = \sum_x \sum_y (\mathbf{I}(x,y) \cdot x^i \cdot y^j), \tag{1}$$

$$m_{00} = \sum_x \sum_y \big(\mathbf{I}(x,y)\big). \tag{2}$$

where $x$ and $y$ are coordinates of the pixels, and $I(x,y)$ are their intensities.

Moments $m_{00}$ , representing the areas of the contours, are compared for three thresholding variants. If the areas are comparable, the contour of the largest area is further used. If the area of the smallest and the largest areas differ more than two times, the curve outlining the smallest area is further used.

At this stage, the number of points describing the contour is related to the resolution of the image and the size of the cross-section. To ensure constant number of points along each of the curves (here, $Np$ = 50) and the same orientation of first point on the curve, B-spline is spanned over the points on the contour and evaluated at given number of points (Fig. 4, left) [20]. With the same topology for each curve and for every

patient, spanning a mesh of quads forming 3D surface models for modal decomposition is straightforward, based on connecting corresponding nodes of neighboring curves. These quads are later divided into triangles (Fig. 4, right) and saved for further analysis.

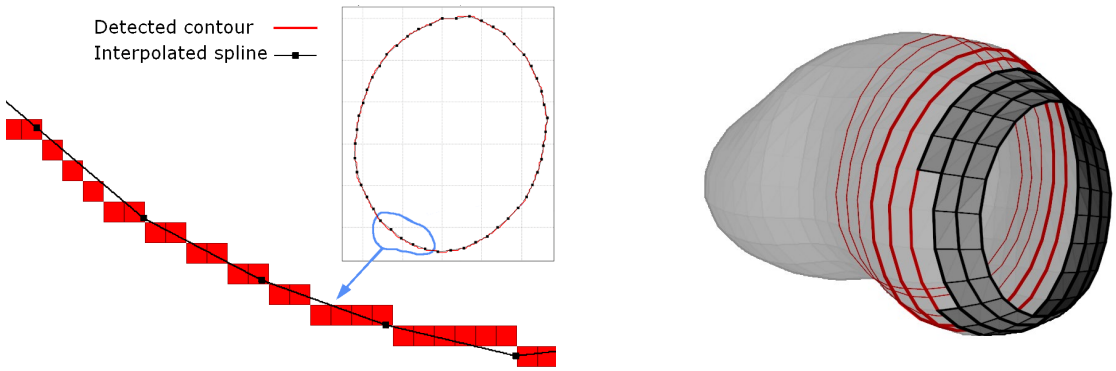


**Figure 4.** B-spline describing the left ventricle on a slice, based on the pixels forming contour (left) and spanning a mesh of triangles using neighboring splines (right).

### 2.3. Principal Component Analysis

Modal decomposition is a very powerful tool used in medical, biomechanical and biometric applications [21]. It reduces the dimension of the data and separates the spatial and temporal/individual variations, simplifying the interpretation of analyzed process/population.

The decomposition techniques include PCA - Principal Component Analysis [22, 23] and its variants like method of snapshots [24], Multilinear PCA [25], Sparse PCA [26] and Kernel PCA [27], Linear Discriminant Analysis (LDA) [28], Independent Component Analysis (ICA) [29] and many other, recently developed methods.

PCA, a method the most widely used in model order reduction, is based on the assumption, that there is a correlation between successive snapshots $v(t_j)$ of the data (here: cardiac cycle consisting of $M$ snapshots). The first step in PCA is the computation of time- or ensemble-average $\bar{u}$:

$$\bar{u} = \frac{1}{M}\sum_{j=1}^{M} v(t_j). \tag{3}$$

Next, the vectors describing input data are centered:

$$\acute{v}(t_j) = v(t_j) - \bar{u}, \qquad j = 1 \ldots M. \tag{4}$$

Resulting vectors $\acute{v}(t_j)$ describe the fluctuations/differences between each snapshot and the average. This data is required to compute the autocorrelation matrix $\mathbf{C}$ of size $N \times N$ (where $N$ is a size of each snapshot and is equal to a product of number of used contours and number of points on contour $N_p$ ):

$$\mathbf{C} = \frac{1}{M}\mathbf{S}\mathbf{S}^{\mathrm{T}}, \quad \text{where} \quad \mathbf{S} = [\acute{v}(t_1) \quad \acute{v}(t_2) \quad \ldots \quad \acute{v}(t_M)], \tag{5}$$

is centered data matrix of size $N \times M$ .

PCA modes are eigenvectors u of standard eigenproblem $\mathbf{C}u = \lambda \mathbf{I}u$, related to eigenvalues $\lambda$ of the largest magnitude. Additionally, temporal coefficients for each mode $i$ and time instant $t_j$ might be computed for whole cardiac cycle from the formula:

$$\alpha_i(t_j) = u_i^T \cdot \acute{v}(t_j). \tag{6}$$

The result of the PCA analysis is a low-dimensional model, consisting of modes, temporal coefficients and eigenvalues corresponding to modes, describing input data using formula:

$$v(t_j) = \bar{u} + \sum_{i=1}^{M} \alpha_i(t_j)\, u_i \;\approx\; \bar{u} + \sum_{i=1}^{N_{mod}} \alpha_i(t_j)\, u_i. \tag{7}$$

Using reduced number of modes $N_{\mathrm{mod}} < M$, the input data is reconstructed with some error. The eigenvalues allow determining the weight of individual features (modes) in the examined set, select the

ones that are required for precise modelling and neglect the least important ones. This way, Principal Component Analysis acts as a filter removing noise and the temporal artifacts, which makes possible to create model, which is both satisfyingly accurate and low-dimensional.

It should be noted that PCA analysis by definition leads to the presentation of (correlated) input data using a minimum number of uncorrelated modes, which makes it useful for model order reduction, belonging to unsupervised machine learning methods. This method of decoupling time and space means that individual forms of heart movement (contraction, translation, rotation and torsion, as specified in [30]) can occur (to varying degrees) within each PCA mode.

Principal Component Analysis has been already used in cardiology. Ghorbanian et al. [31] decomposed the signals from electrocardiography in order to detect the heart arrhythmia. Similar approach has been used by Martis et al. [32] for automated diagnosis of cardiac health. In a paper by Garate-Escamila et al. [33], PCA is used in the process of classification of heart diseases. Input data, coming from UCI Machine Learning Repository [UCI], consists in 74 features resulting from medical interviews and examinations - like pain type and location, details on cigarette smoking, blood pressure, heart rate, etc.

Recently, 4D models are used as an input. Perperidis et al. [34] use POD to analyze cardiac MR and CT image sequences and to classify pulmonary hypertension, and Wu et al. [35] use POD to analyze time-varying, three-dimensional data from ECG-gated multislice cardiac CT images. Przybyła et al. [14] performed PCA for separate patients of SCD dataset.

## 3. Results

In the present paper, PCA is performed on input dataset representing left ventricles of all 45 patients from SCD, with healthy hearts, with hypertrophy and with heart failure. Each ventricle in the (registered) dataset is described by 15 contours (curves), each defined by 24 points, lying on subsequent ‘‘slices’’. The topology of the contours is the same for each curve and each patient. The variables are the coordinates of the points, which differ for individual patients and phases of the heart cycle. These variables are used in modal analysis.

The modes are computed using Tridiagonal QL Implicite (TQLI) algorithm [36]. Eigenvalues of the autocorrelation matrix C, after the normalization:

$$\acute{\lambda}_i = \frac{\lambda_i}{\sum_j \lambda_j} \cdot 100\%, \tag{8}$$

represent part of variance explained by each of the PCA modes. As shown in Fig. 5, the most of the information about the movement of the left ventricle is covered by the first PCA mode (related to the largest eigenvalue) - it explains 68.42% of the variance.

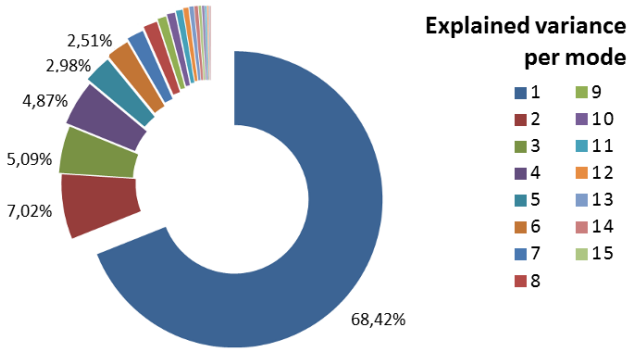


**Figure 5.** Normalized eigenvalues of autocorrelation matrix, representing variance in SCD dataset, explained by the modes.

The second mode explains 7.02% of variance (that is one order of magnitude smaller), and the first three PCA modes are enough to explain 80.52% of total variance of input data. To explain 90%, 95% and 99% of the variance, respectively 6, 9 and 19 modes should be evaluated. The first five PCA modes, superimposed on the cycle-averaged geometry of the left ventricle, are depicted in Fig. 6. Each mode is presented in two extreme positions, resulting from the maximum and minimum values of the temporal coefficients $\alpha_i$ $(t)$ for that mode over whole dataset. It can be seen, that the first mode primarily represents contraction and the changing of ventricle’s volume. Further modes describe more complex movement, related to rotation,

elongation, bending, translation along the cardiac (LV) long axis, and so on. Their importance in the reconstruction of the heart cycle is, as already mentioned, diminishing.

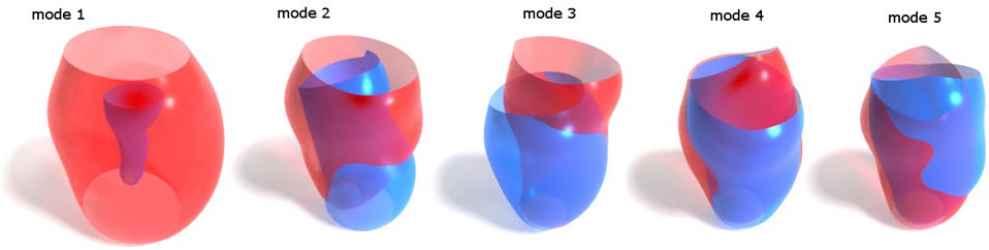


**Figure 6.** The five most dominant PCA modes for SCD dataset, multiplied by the maximum (red) and minimum (blue) values of the temporal coefficients and superimposed on the average geometry.

Thanks to Principal Component Analysis performed on 3D+t data of all patients together, heart cycles might be evaluated by their temporal coefficients. In order to facilitate the analysis of the results, the mean $\bar{\alpha}_i$ (cycle-average) and amplitude $A(\alpha_i)$ were determined for every temporal coefficient for all the patients:

$$\bar{\alpha}_i = \frac{1}{20}\sum_{j=1}^{20} \alpha_i(t), \qquad A(\alpha_i) = max_t\big(\alpha_i(t)\big) - min_t\big(\alpha_i(t)\big). \tag{9}$$

Next, they were used to normalize the course of temporal coefficients:

$$\acute{\alpha}_i(t) = \frac{\alpha_i(t) - \bar{\alpha}_i}{A(\alpha_i)} \cdot 100. \tag{10}$$

As a result, the coefficients for individual patients from different groups (presented for the first mode in Fig. 7) follow a similar course, generally reaching maximum between fifth and twelfth snapshot, and minima on the beginning and at the end of the measured cycle, and the patients might be compared based only on the values of the mean $\bar{\alpha}_i$ (cycle-average) and amplitude $A(\alpha_i)$.

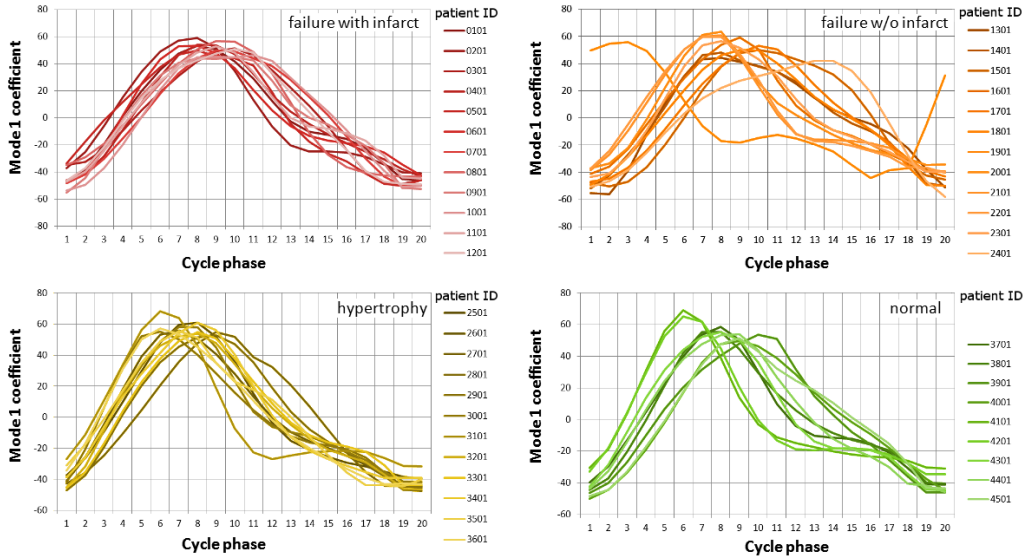


**Figure 7.** Normalized temporal coefficients for the first PCA mode for patients: with heart failure with infarct (top left) and without it (top right), hypertrophy (bottom left) and healthy hearts (bottom right).

A distinction between the groups of the patients can be made by comparing the mean and amplitude values of temporal coefficients for PCA modes. Since the first mode is the most responsible for the change in the volume of the left ventricle, which is used in the calculation of left ventricular ejection fraction (LVEF), it is expected that the corresponding temporal coefficient will be the most useful in distinguishing healthy hearts from the failure ones.

The values of mean values and amplitudes of the first mode's temporal coefficients are presented in Fig. 8. It can be seen from this figure that these characteristics of the first mode's temporal coefficient enable distinguishing patients with heart failure (with and without infarct) from the ones with healthy hearts and with hypertrophy.

In general, patients with healthy hearts and the ones with hypertrophy are characterized by higher values of cycle-average (horizontal axis) and amplitude of temporal coefficient for the first PCA mode. Some cases that might be questionable are marked with letters A-F, where A and B represent patients no 0601 and 1101 with heart failure with infarct, C, D and E represent patients with heart failure without infarct and F represents patient 3601 with hypertrophy. These cases will be discussed later.

Distinguishing between healthy and hypertrophic hearts, as well as between heart failure with and without infarction, does not seem possible based on the temporal coefficients of the first PCA mode. Analysis of temporal coefficients for further modes (and, especially, their cycle-averages and amplitudes, presented in Fig. 9) show no clear linear correlation between these values and the health condition. Cycle-averages and amplitudes of temporal coefficients for the second and the third PCA mode reach different values across the range, regardless of the group to which the patient belongs.

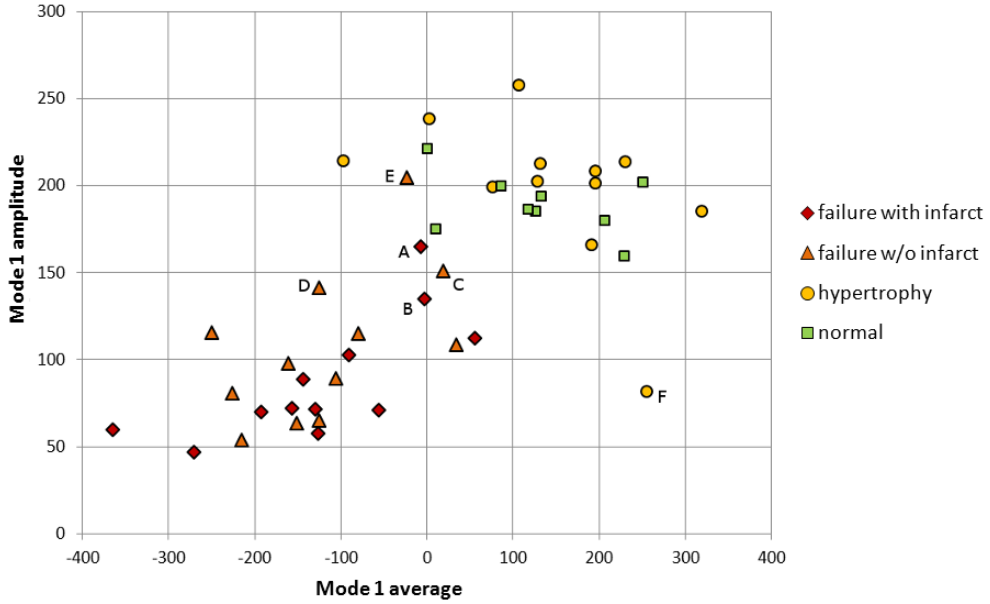


**Figure 8.** Cycle-average and amplitude values of temporal coefficients for the first PCA mode. The symbols: diamonds, triangles, circles and squares (filled with colors according to Fig 6), represent patients with heart failure with and without infarct, with hypertrophy and with healthy hearts, respectively.

To explain the questionable cases (marked A-F in figures 8 and 9), left ventricular ejection fractions (LVEFs) have been computed. LVEF is defined as a stroke volume (difference between end diastolic (EDV) and end systolic (ESV) volumes) of the left ventricle, referred to end diastolic volume and is presented as a percentage:

$$LVEF = \frac{EDV - ESV}{EDV} \cdot 100\%. \tag{11}$$

This parameter, due to the simplicity of obtaining it using any cardiac imaging technique, is commonly used to evaluate patients with heart failure. However, as mentioned in [37], LVEF has some limitations, including the lack of correlation between it and patients' symptoms, and the possibility of heart failure with normal levels of LVEF (> 50%).

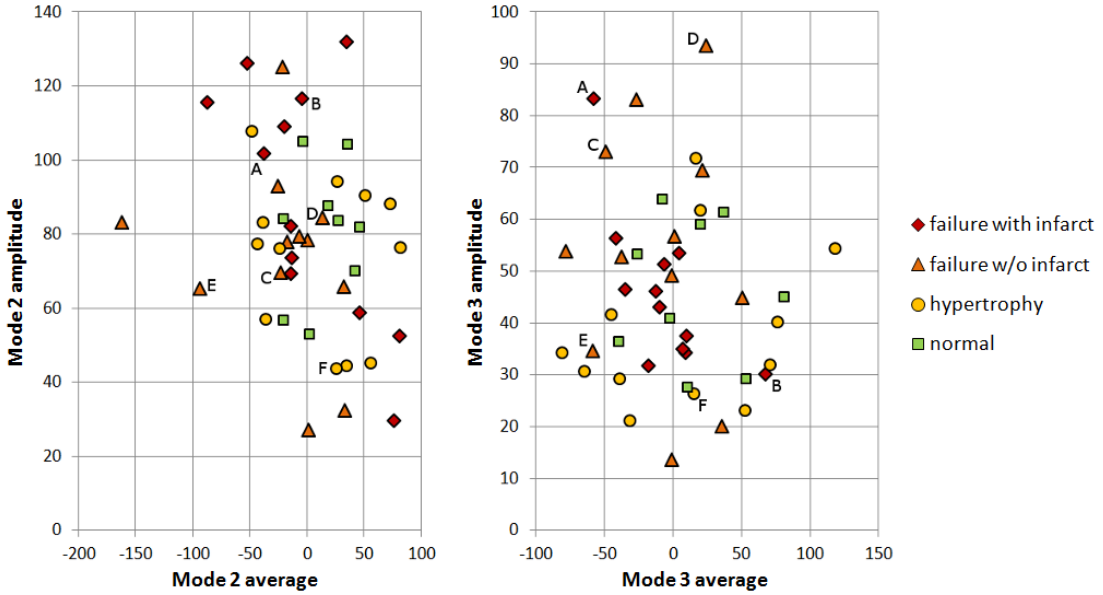


**Figure 9.** Cycle-averages and amplitudes of temporal coefficients for the second and the third PCA modes.

For the computation of volumes of left ventricle 3D models, obtained in this work, the algorithm proposed by Zhang and Chen [38] was used, based on the computation of volumes of tetrahedra formed from triangles on the model's surface and a point lying in a chosen origin.

Table 1 shows group statistics written as average and (in parenthesis) standard deviation, calculated for registered 3D models, referred to the values from Sunnybrook Cardiac Atlas (available on https://www.cardiacatlas.org/).

**Table 1.** End diastolic and systolic volumes (average and – in parenthesis - standard deviations) for subsequent groups of patients: with heart failure with infarct (HF-I), with heart failure without infarct (HF), with hypertrophy and normal, healthy hearts, resulting from this study and following SCD set.

| Patient group | HF-I | HF | Hypertrophy | Normal |
|---|---|---|---|---|
| This study | | | | |
| End Diastolic Volume (ml) | 244.5 (86.1) | 233.0 (61.5) | 113.7 (50.2) | 113.9 (37.7) |
| End Systolic Volume (ml) | 172.4 (89.4) | 155.6 (57.2) | 42.0 (24.3) | 42.1 (15.5) |
| SCD Cardiac Atlas | | | | |
| End Diastolic Volume (ml) | 244.9 (86.0) | 233.7 (63.2) | 114.4 (50.5) | 115.7 (36.9) |
| End Systolic Volume (ml) | 174.3 (90.6) | 158.3 (56.3) | 43.1 (24.5) | 43.1 (14.7) |

It can be seen, that the values used to compute stroke volume are statistically very similar to the SCD data, which allows to conclude on the correctness of the registration and generation of 3D models.

Left ventricular ejection fractions, computed for each patient, are presented in Fig. 10. Colors represent patient groups in a previously adopted manner, and the background of the plot is darkened to highlight preserved LVEF (> 50%), mid-range LVEF (40 – 49%) and reduced LVEF (< 40%) - a classification proposed by the European Society of Cardiology.

On the plot, questionable cases as marked as well. It can be seen, that patients A (0601) and B (1101) from the group with heart failure with infarct, as well as the patients C (2001), D (2101) and E (2201) from the group without infarct, all have relatively high values of LVEF, close to 50%. It is particularly evident for patient E (2101), for whom the amplitude of first PCA mode's temporal coefficient suggested belonging to group of patients with normal hearts
or with hypertrophy.

On the other hand, patient F (3601, hypertrophic) has a lower amplitude of first PCA mode's coefficient than the rest of the normal and hypertrophic patients, corresponding to the values for patients with heart failure. This patient's LVEF, as presented in Fig. 10, is equal to 40.9%.

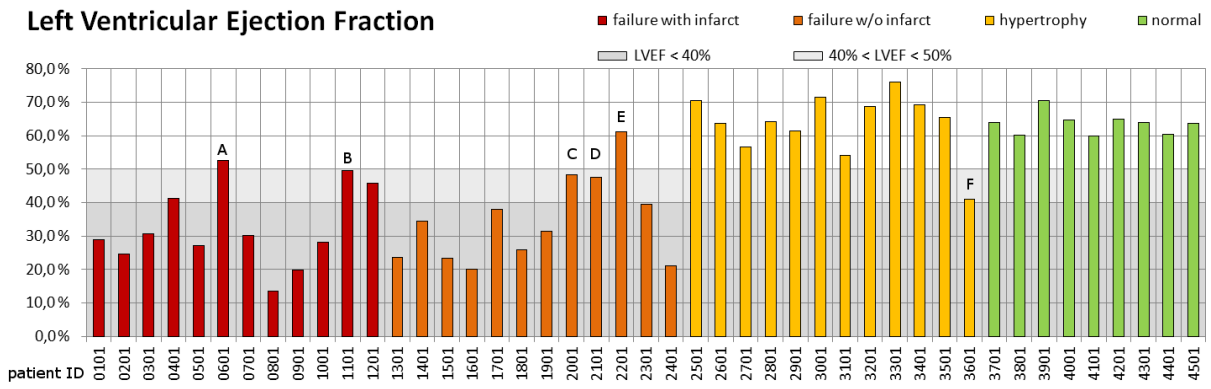


**Figure 10.** Left Ventricular Ejection Fractions (LVEFs) calculated for reconstructed 3D models.

## 4. Discussion and Conclusions

Data from SCD collection has been processed and registered, allowing the design of 4D (spatio-temporal) models of human left ventricles. These models have been decomposed using Principal Component Analysis. As a result, PCA modes, eigenvalues and temporal coefficients, constituting low-dimensional LV models, have been obtained. Basing on the first three modes, it is possible to describe 80.52% of the variance among SCD dataset, and the first mode, representing systolic-diastolic change of volume of the ventricle, is especially useful in diagnosis support.

It has been shown, that the amplitudes and mean values of the coefficient corresponding to the most dominant (first) PCA mode might be used to distinguish patients with healthy hearts and with hypertrophy (higher values) from the ones with heart failure (lower values) and can significantly support the preliminary diagnosis.

These values for these two groups of patients are almost separable – for the analyzed group of 24 patients with heart failure from SCD database, only one (''E'', with ID 2201) had values indicating belonging to a group of healthy patients. It must be stated, that this patient has preserved LVEF (equal to 61%). Another disputable cases include patient with hypertrophy without reported heart failure(''F'', ID 3601) characterized by LVEF equal to 40.9% and three patients with heart failure (''A'' - 0601, ''B'' - 1101 and ''C'' - 2001) with LVEF close to 50%. Such disputable cases might require closer observation and tracking of health by specialists, as they might be related to issues with leading impulses in the conductive system starting the systole and a delay of diastole or systole within the muscle segment [14].

The presented approach was applied to data covering a single heart cycle of each patient. This obviously made it impossible to analyze the temporal changes in the heart cycle associated with illness and high physical exertion. However, such data may not be obtainable with MR imaging.

The correctness of the algorithm requires correct segmentation and data registration, so that the grids corresponding to the surface of the left ventricle at individual moments of the heart cycle, for all patients, have the same topology. The correctness of these operations may be adversely affected by poor quality medical imaging data, which may prevent automatic determination of the left ventricle.

The obtained results correspond to the conclusions presented in [14]. However, the modal analysis of the entire SCD set presented now has some advantages over the previous approach. PCA modes are the same for all patients and their share differences can be interpreted, focusing solely on temporal coefficients and their derivatives. It is also potentially easier to observe the abnormal heart movement - which may result in increased amplitudes of the coefficients for further modes.

Importantly, the three-dimensional movement of the left ventricle, reconstructed by the method described in this paper, contains information often not visible in the conventional 2D data most commonly used in live-time diagnostics. In the opinion of cardiologists [14], these may not reflect the type and cause of the problem, and PCA analysis may enable the identification of abnormalities impossible to observe in 2D images, as well as link them to known diseases before ay dysfunctions or first symptoms appear. This would help prevent changes in the myocardium through early diagnosis and pharmacological or surgical treatment. The main meaning of this work is that, being a non-invasive method, it enables the diagnosis of various hearts, including prenatal ones.

Another application of the procedures presented in this paper is the preparation of the data for machine learning: PCA modes significantly reduce the size of feature vectors, and OpenCV-based registration accelerates the generation of labels.

**Acknowledgments**

This work was supported by a grant of the Ministry of Science and Higher Education in Poland no 0612/SBAD/3576.

**Additional information**

The author(s) declare: no competing financial interests and that all material taken from other sources (including their own published works) is clearly cited and that appropriate permits are obtained.

**References**

1. Eurostat; Deaths from cardiovascular diseases; Technical report, European Union, 2018, https://ec.europa.eu/eurostat/statistics-explained/index.php/Cardiovascular_diseases_statistics; (accessed on 20.09.2021)
2. J. P. Greenwood, N. Maredia, J. F. Younger, et al.; Cardiovascular magnetic resonance and single-photon emission computed tomography for diagnosis of coronary heart disease (ce-marc): a prospective trial; Lancet, 2012, 379(9814), 453-60
3. F. von Knobelsdorff-Brenkenhoff, J. Schulz-Menger; Role of cardiovascular magnetic resonance in the guidelines of the European society of cardiology; J. Cardiovasc. Magnetic. Reson., 2016, 18(1), 6
4. M. A. Viergever, J. B. A. Maintz, S. Klein, K. Murphy, M. Staring, J. P. W. Pluim; A survey of medical image registration - under review; Med. Image Anal., 2016, 33, 140-144
5. S.K. Zhou., H. Greenspan, D. Shen; Deep learning for medical image analysis; Academic Press, Elsevier, 2017
6. J. Ker, L. Wang, J. Rao, T. Lim; Deep learning applications in medical image analysis; IEEE Access 2017, 6, 9375-9389
7. H. Hu, N. Pan, J. Wang, T. Yin, R. Ye; Automatic segmentation of left ventricle from cardiac MRI via deep learning and region constrained dynamic programming; Neurocomputing, 2019, 347, 139-148
8. L.K. Tan, R.A. McLaughlin, E. Lim, Y.F. Abdul Aziz, Y.M. Liew; Fully automated segmentation of the left ventricle in cine cardiac MRI using neural network regression; J. Magn. Reson. Imaging, 2018, 48(1), 140-152
9. C.D. Kemp, J.V. Conte; The pathophysiology of heart failure; Cardiovasc. Pathol., 2012, 21(5), 365-371
10. Mayo Clinic. Diseases and conditions; https://www.mayoclinic.org/diseases-conditions/; 2021, (accessed on 20.09.2021)
11. F. Van de Werf, J. Bax, A. Betriu, et al; Management of acute myocardial infarction in patients presenting with persistent st-segment elevation: the task force on the management of st-segment elevation acute myocardial infarction of the european society of cardiology; Eur. Heart J., 2008, 29(23), 2909-2945
12. M. Yildiz, A.A. Oktay, M.H. Stewart, R.V. Milani, H.O. Ventura, C.J. Lavie; Left ventricular hypertrophy and hypertension; Prog. Cardiovasc. Dis., 2020, 63(1), 10-21
13. P. Radau, Y. Lu, K. Connelly, G. Paul, A.J. Dick, G.A. Wright; Evaluation framework for algorithms segmenting short axis cardiac MRI; MIDAS J - Cardiac MR Left Ventricle Segmentation Challenge, 2009, 49; Dataset is available at: https://www.cardiacatlas.org/sunnybrook-cardiac-data/
14. P. Przybyła, W. Stankiewicz, M. Morzyński, M. Nowak, D. Gaweł, S. Stefaniak, M. Jemielity; Reduced order model of a human left and right ventricle based on POD method. In: Computational Biomechanics for Medicine: From Algorithms to Models and Applications; A. Wittek, G. Joldes, P.M.F. Nielsen, B.J. Doyle, K. Miller, editors; Springer, Cham, 2017, 57-69
15. G. Bradski, A. Kaehler; Learning OpenCV: Computer vision with the OpenCV library; O'Reilly Media Inc., 2008
16. P. Dierckx; Curve and surface fitting with splines; Oxford University Press: Oxford, 1995
17. P. Perona, J. Malik; Scale-space and edge detection using anisotropic diffusion; IEEE Trans. Pattern Anal. Mach. Intell., 1990, 12(7), 629-639
18. T. S. Huang, G. J. Yang, G. Y. Tang; A fast two-dimensional median filtering algorithm; IEEE Trans. Acoust., 1979, 27(1), 13-18
19. S. Suzuki, K. Abe; Topological structural analysis of digitized binary images by border following; Comput. Vis. Graph. Image Process., 1985, 30(1), 32–46
20. E. Jones, T. Oliphant, P. Peterson; SciPy: Open source scientific tools for Python; https://www.scipy.org; 2021

21. M. Rychlik, W. Stankiewicz, M. Morzyński; Numerical analysis of geometrical features of 3D biological objects, for three-dimensional biometric and anthropometric database; In: UAHCI 2011. Lecture Notes in Computer Science; Stephanidis C., editor; Springer, Berlin-Heidelberg, 2011, 6766, 108-117
22. N. Aubry, R. Guyonnet, R. Lima; Spatiotemporal analysis of complex signals: Theory and applications; J. Stat. Phys., 1991, 64(2/3), 683-739
23. G. Berkooz, P. Holmes, Lumley JL; The proper orthogonal decomposition in the analysis of turbulent flows; Ann. Rev. Fluid Mech., 1993, 25(1), 539–575
24. L. Sirovich; Turbulence and the dynamics of coherent structures; Q. Appl. Math., 1987, 45, 561-571
25. H. Lu, K.N. Plataniotis, A.N. Venetsanopoulos; MPCA: Multilinear principal component analysis of tensor objects; IEEE Trans. Neural. Netw., 2008, 19(1), 18-39
26. H. Zou, T. Hastie, R. Tibshirani; Sparse principal component analysis; J. Comput. Graph. Stat., 2006, 15(2), 265-286
27. H. Hoffmann; Kernel PCA for novelty detection; Pattern Recognition 2007, 40, 863-874
28. H. Yu, J. Yang; A direct LDA algorithm for high-dimensional data - with application to face recognition; Pattern recognit., 2001, 34(10), 2067–2070
29. A. Hyvärinen, O. Erkki; Independent component analysis: algorithms and applications; Neural Netw., 2000, 13(4-5), 411-430
30. S. Nakatani; Left ventricular rotation and twist: why should we learn?; J Cardiovasc Ultrasound, 2011, 19(1), 1-6
31. P. Ghorbanian, A. Ghaffari, A. Jalali, C. Nataraj; Heart arrhythmia detection using continuous wavelet transform and principal component analysis with neural network classifier; In: Computing in Cardiology, IEEE, 2010, 669–672
32. R. J. Martis, U. R. Acharya, K. M. Mandana, A. K. Ray, C. Chakraborty; Application of principal component analysis to ECG signals for automated diagnosis of cardiac health; Expert Syst. Appl., 2012, 39(14), 11792-11800
33. A. K. Gárate-Escamila, A. H. El Hassani, E. Andrès; Classification models for heart disease prediction using feature selection and PCA; Inform. Med. Unlocked, 2020, 19, 100330
34. D. Perperidis, R. Mohiaddin, P. Edwards, D. Rueckert; Segmentation of cardiac MR and CT image sequences using model-based registration of a 4D statistical model; Medical imaging 2007: Image Processing, 2007, 6512:65121D
35. J. Wu, Y. Wang, M. A. Simon, J. C. Brigham; A new approach to kinematic feature extraction from the human right ventricle for classification of hypertension: a feasibility study; Physics in Medicine and Biology, 2012, 57(23), 7905-7922
36. W. H. Press, S. A. Teukolsky, W. T. Vetterling, B. P. Flannery; Numerical Recipes in C: The Art of Scientific Computing, second edition; Cambridge University Press, Cambridge, MA, 1992
37. D. Mele, M. Nardozza, R. Ferrari; Left ventricular ejection fraction and heart failure: an indissoluble marriage?; Eur. J. Heart Fail., 2018, 20, 427-430
38. C. Zhang, T. Chen; Efficient feature extraction for 2D/3D objects in mesh representation; In: Proceedings of 2001 International Conference on Image Processing (Cat. No. 01CH37205), vol. 3; Institute of Electrical and Electronics Engineers, 2001, 935-938